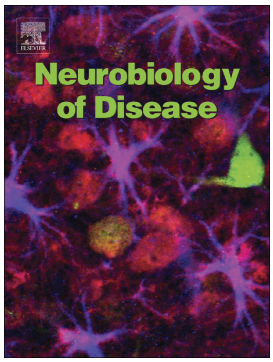

cJun N-terminal kinase (JNK) mediates cortico-striatal signaling in a model of Parkinson's disease

Giada Spigolon, Anna Cavaccini, Massimo Trusel, Raffaella Tonini, Gilberto Fisone

PII: S0969-9961(17)30243-7
DOI: doi:10.1016/j.nbd.2017.10.015
Reference: YNBDI 4054

To appear in: *Neurobiology of Disease*

Received date: 7 September 2017
Revised date: 23 October 2017
Accepted date: 27 October 2017

Please cite this article as: Giada Spigolon, Anna Cavaccini, Massimo Trusel, Raffaella Tonini, Gilberto Fisone , cJun N-terminal kinase (JNK) mediates cortico-striatal signaling in a model of Parkinson's disease. The address for the corresponding author was captured as affiliation for all authors. Please check if appropriate. Ynbdi(2017), doi:10.1016/j.nbd.2017.10.015

cJun N-terminal kinase (JNK) mediates cortico-striatal signaling in a model of Parkinson's disease

Abbr. title: JNK mediates dopamine receptor transmission at corticostriatal synapses

Giada Spigolon[1*], Anna Cavaccini[2*], Massimo Trusel[2], Raffaella Tonini[2#], Gilberto Fisone[1#]

[1]*Department of Neuroscience, Karolinska Institutet, 171 77 Stockholm, Sweden;* [2]*Neuroscience and Brain Technologies Department, Istituto Italiano di Tecnologia, 16163 Genova, Italy.*

* Co-first authors

Co-senior corresponding authors

Corresponding authors:

Gilberto Fisone

Department of Neuroscience

Karolinska Institutet

Retzius väg 8

17177 Stockholm

Sweden

e-mail: gilberto.fisone@ki.se

Raffaella Tonini

Department of Neuroscience and Brain Technologies

Istituto Italiano di Tecnologia

Via Morego 30

16145 Genova, Italy

e-mail: raffaella.tonini@iit.it

Abstract

The cJun N-terminal kinase (JNK) signaling pathway has been extensively studied with regard to its involvement in neurodegenerative processes, but little is known about its functions in neurotransmission. In a mouse model of Parkinson's disease (PD), we show that the pharmacological activation of dopamine D1 receptors (D1R) produces a large increase in JNK phosphorylation. This effect is secondary to dopamine depletion, and is restricted to the striatal projection neurons that innervate directly the output structures of the basal ganglia (dSPN). Activation of JNK in dSPN relies on cAMP-induced phosphorylation of the dopamine- and cAMP-regulated phosphoprotein of 32 kDa (DARPP-32), but does not require N-methyl-D-aspartate (NMDA) receptor transmission. Electrophysiological experiments on acute brain slices from PD mice show that inhibition of JNK signaling in dSPN prevents the increase in synaptic strength caused by activation of D1Rs. Together, our findings show that dopamine depletion confers to JNK the ability to mediate dopamine transmission, informing the future development of therapies for PD.

Key words: dopamine, striatum, mouse, long-term depression, Parkinson´s disease, L-DOPA

Introduction

Dopamine transmission is involved in numerous basic physiological processes and its abnormal activity is characteristic of several neuropsychiatric and neurodegenerative disorders, including drug addiction and Parkinson's disease (PD). Dopamine's effects are enacted through binding to two major types of G-protein coupled receptors, the D1 (D1R) and D2 (D2R) receptors, which are linked to stimulation and inhibition of cAMP signaling, respectively [1].

In experimental models of PD, the loss of dopaminergic afferents to the striatum is associated with sensitized dopamine transmission. Previous work shows that this sensitization is particularly prominent for D1Rs [2,3], which are selectively expressed in the striatal projection neurons (SPNs) that form the direct pathway to the output nuclei of the basal ganglia [4]. D1R sensitization in response to dopamine depletion has been attributed to abnormal recruitment of D1Rs at the cell surface, as well as increased levels of G_{olf} and adenylyl cyclase [5-8]. These changes dramatically enhance the effects produced by dopaminergic drugs on cAMP signaling [9]. In addition, sensitized D1R transmission confers on L-DOPA, the most commonly prescribed medication for PD, the ability to activate non-canonical signal transduction pathways, such as the extracellular signal-regulated kinases (ERK) and the mammalian target of rapamycin [9-14]. Whether activation of sensitized D1Rs also leads to the stimulation of other downstream targets in SPNs remains to be established.

The cJun N-terminal kinase (JNK) signaling pathway is a member of the mitogen-activated protein kinase family, which has been extensively studied with regard to cell survival and proliferation. The primary target of JNK is the early response transcription factor, cJun, which is a component of the adaptor protein-1 (AP-1) [15,16]. JNK-mediated phosphorylation enhances the transcriptional efficiency of cJun by increasing its binding to DNA at promoter sites [17,18]. Work in human neuroblastoma cells showed that D1Rs activate JNK via stimulation of cAMP-dependent protein kinase [19]. Moreover, repeated administration of cocaine, a drug which acts by promoting dopamine transmission, results in a

transient increase in the phosphorylation of JNK [20]. However, despite the potential clinical implications, virtually nothing is known on the role of JNK in dopamine transmission in PD.

To address this question, we investigated whether striatal JNK mediates the cellular and synaptic effects of D1R activation in naïve mice and in the 6-hydroxydopamine (6-OHDA) mouse model of PD. We find that activation of D1Rs with a specific agonist or L-DOPA increases the phosphorylation of JNK and cJun in SPNs that project directly to the output nuclei of the basal ganglia (dSPN). This effect is observed in concomitance with dopamine depletion, which is one of the cardinal features of PD, and is mediated by cAMP-dependent phosphorylation of dopamine- and cAMP-regulated phosphoprotein of 32 kDa (DARPP-32). Finally, we show that JNK is involved in the D1R-mediated regulation of synaptic mechanisms of plasticity at cortico-striatal synapses on dSPN in the disease state, but not under physiological conditions.

Materials and Methods

Animals

C57BL/6J mice (3 months old, 25-30 g) were purchased from Charles River Laboratories (Netherlands). *Drd1a*-EGFP and *Drd2*-EGFP mice were generated by the GENSAT (Gene Expression Nervous System Atlas) program at the Rockefeller University [21]. T34A DARPP-32 mutant mice were generated as described in [22]. All transgenic mice were backcrossed on a C57BL/6 background for at least ten generations. Animals were maintained in a 12-h light-dark cycle, in stable conditions of temperature (22°C), with food and water *ad libitum*. All experiments had received prior approval by the local animal ethical committee, Stockholms Norra Djurförsöksetiska Nämnd, and were carried out in accordance with the European Community Council Directive of 24 November 1986 (86/609/EEC).

Drugs

Drugs were dissolved in saline and injected intraperitoneally in a volume of 10 ml/kg of body weight. L-DOPA (Sigma Aldrich) (10 mg/kg) was administered in combination with the peripheral DOPA decarboxylase inhibitor, benserazide hydrochloride (Sigma Aldrich) (7.5 mg/Kg). SCH23390 (Abcam) (0.2 mg/Kg) and MK-801 (Tocris) (0.15 mg/Kg) were injected 15 and 30 min prior to L-DOPA, respectively. SKF38393 (Tocris) was administered at the dose of 10 mg/Kg. For the electrophysiological experiments, DPCPX (500 nM, Tocris), L-DOPA (10 µM, Tocris), SKF38393 (3µM Tocris) were bath applied during the recoding, as indicated in the corresponding figure. SP600125 (Tocris) was dissolved in DMSO and used at the final concentration of 10 µM in the pipette solution. JNK-IN-8 (Selleck Chemicals) stock solution was prepared in DMSO, and used at the final concentration of 1 µM. Control solutions for the experiments with JNK inhibitors always contained the corresponding DMSO concentration (up to 0.1%).

6-OHDA lesion

In order to deplete dopamine in the right striatum, mice were injected with 6-hydroxydopamine-HCl (6-OHDA; Sigma-Aldrich, Sweden AB) into the ipsilateral medial forebrain bundle (MFB). All animals received subcutaneous injections of Temgesic® as analgesic at a dose of 0.1 mg/kg, before the surgical procedure. Anesthesia was induced with 4% isofluorane and maintained with 2% isoflurane. The mouse was positioned in a stereotaxic frame (David Kopf Instruments, Tujunga, CA) on a heating pad to maintain normothermia. 6-OHDA was dissolved in 0.02% ascorbic acid in saline at a concentration of 3.75 µg of free-base 6-OHDA per microliter. Each mouse was injected with 1 µl (0.2 µl /min) of solution into the right MFB according to the following coordinates (mm): anteroposterior (AP), -1.2; mediolateral (ML), -1.2; dorsoventral (DV), -4.8 (all millimeters relative to bregma). The needle was left in place for 5 min before and after injection. Mice were allowed to recover for 3 weeks before experimentations. The 6-OHDA lesion was evaluated by immunofluorescence for tyrosine hydroxylase (TH); only animals with a reduction of TH immunoreactivity of 85% or more were included in the study.

Immunofluorescence

At the indicated times after drug treatments, mice were deeply anesthetized with sodium pentobarbital (200 mg/kg, i.p., Sanofi-Aventis, France) and perfused transcardially with 4% (weight/vol) ice-cold paraformaldehyde in 0.1M phosphate buffer. The brains were post-fixed overnight in the same solution and 40 µm-thick coronal sections were cut with a Vibratome (Leica, Germany). Immunolabeling for phospho-JNK was performed using the tyramide signal amplification (TSA) protocol with an anti-phospho JNK antibody (1:100; 9251, Cell Signalling Technology, Sweden) detected with an HRP-conjugated secondary antibody (Dako, Glostrup, Denmark) and Cy3-conjugated tyramide (1:500; Perkin Elmer; Waltham, MA, USA). Phospho-cJun was visualized using an anti-phospho cJun primary antibody raised against phospho-Ser73-cJun (1:100; 9164, Cell Signalling Technology, Sweden) and a Cy3-

conjugated secondary antibody (1:400, Jackson Laboratories). In a subset of experiments, phospho-cJun was also visualized using an antibody against phospho-Ser63-cJun with undistinguishable results (data not shown). A primary antibody against EGFP (1:1000; Aves labs, Tigard, OR, USA) and a 488-conjugated secondary antibody (1:500; Life Technologies, Paisley, UK) were used to visualize EGFP. Triple-labeling for P-JNK/P-cJun/EGFP was performed as described in [23]. Briefly, P-JNK staining was carried out using the TSA technique and microwave treatment of the sections was performed before proceeding with the P-cJun/EGFP staining. Immunofluorescence against TH was carried out using an anti-TH primary antibody (1:500, AB152, Millipore) and a Cy3-conjugated secondary antibody (1:400, Jackson Laboratories). Single-, double- and triple-labeled images of the dorsal striatum were captured using sequential laser scanning confocal microscopy (Zeiss LSM, Carl Zeiss, Jena, Germany) at 20, 40 and 63X magnification. Quantification of staining was obtained averaging two 20X images per section, in two sections per animal, by counting positive cells above background using Image J software and the average number of positive cells was reported.

***Ex vivo* slice experiments**

Mice with a unilateral injection of 6-OHDA in the MFB were killed by decapitation and the brains rapidly removed. Coronal slices (250 μm) were prepared using a vibratome (Leica, Germany) and punches corresponding to the dorsal striatum were dissected out from the control, or the 6-OHDA-lesion side. Two punches were placed in individual 5-ml polypropylene tubes containing 2 ml of Krebs-Ring bicarbonate buffer containing 118 mM NaCl, 4.7 mM KCl, 1.3 mM $CaCl_2$, 1.5 mM $MgSO_4$, 1.2 mM KH_2PO_4, 25 mM $NaHCO_3$ and 11.7 mM glucose, aerated with 95% O_2 and 5% CO_2. The samples were equilibrated at 30 °C for 30 min, followed by incubation with either SP600125 (20 μM) or JNK-IN-8 (10 μM) for 15 and 45 min, respectively. SKF38393 (3 μM) was added for 5 min with or without JNK inhibitors. After incubation, the punches were removed and sonicated in 1% SDS for Western blotting analysis.

Western blotting

Aliquotes (5 µl) of the homogenate from the ex vivo slice experiment were used for protein quantification with a BCA assay kit (Pierce, Europe). Proteins were separated by SDS-polyacrylamide gel electrophoresis and transferred overnight to PVDF membranes (Amersham Pharmacia Biotech, Uppsala, Sweden). The following primary antibodies were used: anti-TH (1:2000, AB152, Millipore), anti-phospho-Ser73-cJun (1:500; 9164, Cell Signalling Technology, Sweden), anti-total-cJun (1:1000; 9165, Cell Signaling Technology, Sweden), anti-phospho ERK 1/2 (1:2000; Cell Signaling Technology, Sweden), anti-total ERK 1/2 (1:2000, Cell Signaling Technology, Sweden), anti-β-actin (1:10000, A5441 Sigma-Aldrich, Sweden).

Acute slice preparation

Mice were anesthetized with isoflurane and decapitated, and their brains were transferred to ice-cold artificial cerebrospinal fluid (aCSF) containing 110 mM choline chloride, 2.5 mM KCl, 1.25 mM NaH_2PO_4, 7 mM $MgCl_2$, 0.5 mM $CaCl_2$, 25 mM $NaHCO_3$, 25 mM D-glucose and 11.6 mM ascorbic acid, saturated with 95% O_2 and 5% CO_2 for dissection. Horizontal slices (270 µm thick) were prepared using a Vibratome 1000S slicer (Leica), then transferred to new aCSF containing 115 mM NaCl, 3.5 mM KCl, 1.2 mM NaH_2PO_4, 1.3 mM $MgCl_2$, 2 mM $CaCl_2$, 25 mM $NaHCO_3$, and 25 mM D-glucose, and aerated with 95% O_2 and 5% CO_2. After incubating for 20 min at 32 °C, slices were kept at 22-24 °C. During experiments, slices were continuously superfused with aCSF at a rate of 2 ml/min at 28 °C.

Electrophysiology

Whole-cell recordings were performed on horizontal brain slices, which preserve intact corticostriatal connections [24]. SPN in the DLS were visualized under infrared-differential interference contrast and were identified on the basis of morphological and electrical properties [25]. After recording, the identity

of the cells was confirmed by immunostaining to measure the expression of substance P (which is expressed in dSPN) and adenosine A2A receptors (which are expressed in the SPN that project indirectly to the output nuclei of the basal ganglia; iSPNs) [26]. Patch pipettes (4-6 MΩ) were filled with a solution containing 130 mM KMeSO4, 5 mM KCl, 5 mM NaCl, 10 mM HEPES, 2 mM MgCl2, 0.1 mM EGTA, 0.05 mM CaCl2, 2 mM Na2ATP and 0.4 mM Na3GTP (pH 7.2-7.3, 280-290 mOsm/kg) and with Neurobiotin (0.5 mg/ml). Excitatory postsynaptic potentials (EPSPs) in the DLS were evoked in presence of the GABAA receptor antagonist gabazine (10 µM) by stimulation of the somatosensory cortex layer 5, and acquired every 10 s. Long-term synaptic depression induced by high-frequency stimulation (HFS-LTD) was generated with 4 × 1-s-long 100 Hz trains repeated every 10 s. During train stimulation, the postsynaptic cell was depolarized from -80 to -50 mV to mimic cortically-induced up-states. Data were excluded when the input resistance (R_{inp}) changed >20%. The occurrence and magnitude of synaptic plasticity was evaluated by comparing the EPSP amplitudes from the last 10 min of baseline recordings with the values at 25-35 min after HFS. LTD plots were generated by averaging the peak amplitude of individuals EPSPs in 2 min bin. After recording, brain slices were fixed with 4% PFA. Antigen retrieval (sodium citrate 50 mM, 30 min, 80 °C) was performed and the slices were incubated with primary antibodies specific for iSPNs (anti-A2A, 1:250, Enzo Biosciences) and for dSPN (anti-substance P, 1:200, Millipore), diluted in 0.1 M PB containing 0.3% (v/v) Triton X-100 and 0.02% NaN_3). Sections were then incubated in Alexa 568-conjugated streptavidin (1:5000; Invitrogen), followed by secondary antibodies (Invitrogen).

Statistics

Biochemical data were analyzed with unpaired, two-tailed t-test, one-way (1W) or two-way (2W) analysis of variance (ANOVA), where lesion and treatment/time/genotype were the independent variables. Electrophysiological data were analyzed by one-way repeated measures (1W RM) ANOVA for comparisons within a group, and by 1W ANOVA for between-group comparisons (GraphPad Instat 6

software). Post hoc analyses (Tukey and Dunnet multiple comparison tests) were only performed for ANOVAs that yielded significant main effects. For comparisons of two groups, an independent two-sample t-test was used.

Results

L-DOPA increases phosphorylation of JNK and cJun in the dopamine depleted, but not in the intact, striatum

C57BL/6J mice with a unilateral 6-OHDA lesion were injected with either saline or L-DOPA (10 mg/kg, i.p.) and changes in the phosphorylation of JNK and cJun were determined after 15, 30, 60, or 120 min. Fig. 1A shows the loss of dopaminergic innervation produced by 6-OHDA, assessed as lack of TH-immunoreactivity in the dorso-lateral striatum (DLS) ipsilateral to the lesion. The 6-OHDA-lesion *per se* did not produce any modification in the state of phosphorylation of JNK (Fig. 1B, upper panels and Fig. 1D, left histogram) and cJun (Fig. 1C, upper panels and Fig. 1E, left histogram). Administration of L-DOPA increased the number of cells immunoreactive for phosphorylated JNK (P-JNK; Fig. 1B, lower panels) ($p < 0.0001$) and cJun (P-cJun; Fig. 1C, lower panels) ($p < 0.0001$), in the DLS ipsilateral to the 6-OHDA-lesion. The effects of L-DOPA on both P-JNK and P-cJun peaked 15 min after injection and returned to near baseline after 120 min (Fig. 1D,E, right line graphs). In contrast, L-DOPA had no effect in the intact DLS, contralateral to the 6-OHDA-lesion (cf. left panels in Fig. 1B,C, and left histograms in Fig. 1D,E).

L-DOPA regulates JNK signaling in the D1R expressing dSPN

To determine whether the effects of L-DOPA were cell-type specific, we examined changes in phosphorylation of JNK and cJun in dSPN, which express D1Rs, and in the iSPNs, which are instead enriched in D2Rs. For this purpose, 6-OHDA was injected in mice expressing EGFP in dSPN (*Drd1a*-

EGFP mice), or iSPNs (*Drd2*-EGFP mice). Mice were then treated with L-DOPA (10 mg/kg, i.p.) and perfused for immunohistochemical analysis 30 min later. In *Drd2*-EGFP mice, L-DOPA-induced phosphorylation of JNK (Fig. 2A, upper panels) and cJun (Fig. 2B, upper panels) was localized in EGFP-negative cells ($p = 0.0002$ for P-JNK and $p = 0.0007$ for P-cJun). Conversely, in *Drd1a*-EGFP mice L-DOPA-induced phosphorylation of JNK (Fig. 2A, lower panels) and cJun (Fig. 2B, lower panels) was largely co-localized with EGFP ($p = 0.0005$ for P-JNK and $p = 0.0012$ for P-cJun). High magnification of the striatum from a *Drd2*-EGFP mouse revealed that P-JNK and P-cJun were increased in the same EGFP-negative SPNs (Fig. 2C). These results indicate that L-DOPA enhances the phosphorylation of JNK and cJun specifically in dSPN.

Pharmacological activation of D1Rs promotes JNK signaling in the dopamine depleted striatum

The selective localization of P-JNK and P-cJun in dSPN suggests that the effect of L-DOPA occurs through the activation of D1Rs, which are highly enriched in this neuronal subpopulation. Consistent with this, the ability of L-DOPA to increase P-JNK in the dopamine depleted striatum was abolished by the D1R antagonist SCH23390 (0.2 mg/kg) (Fig. 3A,B; $p < 0.0001$). Similarly, L-DOPA-induced cJun phosphorylation was markedly decreased by SCH23390 (Fig. 3C,D; $p = 0.0055$).

To confirm the involvement of D1Rs in the regulation of JNK and further assess the impact of dopamine depletion on signaling processes, mice with a unilateral 6-OHDA lesion were treated with the selective D1R agonist, SKF38393 (10 mg/Kg). Administration SKF38393 did not affect P-JNK (Fig. 3E,F) and P-cJun (Fig. 3G,H) in intact striata (i.e. contralateral to the 6-OHDA-lesion). In contrast, SKF38393 induced a large increase in the number of P-JNK (Fig. 3E,F; $p < 0.0001$) and P-cJun (Fig. 2G,H; $p = 0.0001$) immunoreactive cells in the dopamine depleted striata (i.e. ipsilateral to the 6-OHDA-lesion).

L-DOPA-mediated regulation of JNK and cJun requires cAMP signaling via DARPP-32, but is independent of NMDA receptor transmission

In striatal SPNs, one of the primary effects of D1R activation is the phosphorylation of DARPP-32, an inhibitor of protein phosphatase-1 (PP-1) required for cAMP signaling [27]. Therefore, we investigated whether DARPP-32 was required for L-DOPA-induced phosphorylation of JNK and cJun. Mice expressing a mutated form of DARPP-32, which lacks the activating cAMP-dependent protein kinase (PKA) phosphorylation site (Thr34) (T34A DARPP-32 mutant mice), were injected unilaterally with 6-OHDA and treated with L-DOPA. We found that functional inactivation of DARPP-32 decreased the L-DOPA-induced phosphorylation of JNK and cJun (Fig. 4A, B, $p < 0.0001$ for P-JNK; Fig. 4C,D, $p = 0.005$ for P-cJun).

The ability of dopaminergic drugs to activate ERK depends on NMDA receptor transmission [28-30]. Similarly, in brain regions other than the striatum, activation of JNK requires intact glutamate receptors signaling [31]. Therefore, we examined whether NMDA receptors are involved in the effects of L-DOPA. For this purpose, we treated PD mice with L-DOPA or a combination of L-DOPA and the non-competitive NMDA receptor antagonist, MK-801 (0.15 mg/kg). Inhibition of NMDA receptors did not impact the increase in the number of P-JNK- and P-cJun-positive cells induced by L-DOPA in the dopamine depleted striatum (Fig. 4E-H, $p > 0.05$).

In summary, we found that L-DOPA-mediated regulation of the JNK pathway depends on cAMP-mediated phosphorylation of DARPP-32, but does not require activation of NMDA receptors. These results suggest that JNK/cJun signaling may be implicated in cellular responses produced by activation of D1Rs in the PD state.

JNK signaling contributes to D1R-mediated regulation of synaptic plasticity at cortical afferents to dSPN in PD mice.

Data so far point to dSPN acquiring a D1R-mediated, cell-type specific regulation of JNK signaling cascade upon dopamine depletion. Therefore, we tested the possibility that JNK activation can mediate some of the modulatory effects of dopamine at corticostriatal synapses on dSPN in the PD state. In dSPN, we have recently shown that HFS-LTD of cortical afferents is dependent on presynaptic adenosine A1 receptors (A1R) and blunted upon the concurrent activation of postsynaptic D1R [26]. In light of this, we test whether pharmacological manipulations of the JNK signaling interfered with the dopaminergic suppression of HFS-LTD in dopamine depleted striata compared to control striata. In the ipsilateral DLS of mice with a 6-OHDA-lesion, we triggered HFS-LTD at cortical connections to dSPN (Fig. 5A, 6-OHDAipsi, 66 ± 8 % of baseline, $p < 0.05$). LTD was abolished by bath application of the A1R antagonist DPCPX (500 nM) (Fig. 5A, 6-OHDAipsi + DPCPX, 93 ± 6 % of baseline, $p > 0.05$), as previously shown in naive mice [26]. Stimulation of the dopaminergic signaling by L-DOPA (10 µM) or the direct pharmacological activation of the D1R subtype by the agonist SKF38393 (3 µM) significantly impaired LTD in 6-OHDA-lesion mice (Fig. 5B, 6-OHDAipsi + L-DOPA, 88 ± 4 % of baseline, $p > 0.05$; 6-OHDAipsi + SKF, 91 ± 2 % of baseline, $p > 0.05$). We next tested the involvement of JNK in the synaptic effect produced by pharmacological activation of D1R in either 6-OHDA lesioned or naïve mice. In PD mice, we found that including the JNK inhibitor SP600125 (10 µM) in the postsynaptic dSPN during SKF38393 application prevented the synaptic effect of D1R activation (Fig. 6A, 6-OHDAipsi + SKF/SP600125, 71 ± 6 % of baseline, $p < 0.05$). We obtained similar results with the more selective and structurally unrelated JNK inhibitor JNK-IN-8 [32] (1 µM) (Fig. 6A, SKF/JNK-IN-8, 58 ± 1 % of baseline, $p < 0.05$). We also confirmed that the two inhibitors affected SKF38393-induced cJun phosphorylation in the striata of PD mice (Fig. 6B, top panels, SKF/SP600125, $p = 0.0272$; SKF/JNK-IN-8, $p < 0.0001$), without interfering with P-ERK 1/2 phosphorylation (Fig. 6B, bottom panels, SKF/SP600125 and SKF/JNK-IN-8, $p > 0.05$). In naïve mice, SKF38393 still impaired LTD (Fig. 6C, naive, 63 ± 5 % of baseline, $p < 0.05$; naive + SKF, 89 ± 3 % of baseline, $p > 0.05$), as expected from our previous observations [26]. However, inhibition of JNK signaling by JNK-IN-8 failed to reduce the D1R-

mediated synaptic effects (naive + SKF/JNK-IN-8, 90 ± 8 % of baseline, n = 6, $p > 0.05$; Fig. 6C). This is consistent with the lack of D1R-mediated JNK activation in the intact striatum (Fig. 3E-H). After recordings, dSPN cell identity was confirmed by immunostaining for substance P (positive) and A2A (negative) (data not shown) [25]

Together, these results demonstrate that dopamine depletion confers the ability to D1R to signal by JNK, supporting a role for the dopaminergic regulation of the JNK signaling pathway in striatal dysfunction.

Discussion

We have identified the JNK pathway as a signaling mechanism implicated in dopamine transmission, and provide evidence in an experimental model of PD that JNK is required for D1R-dependent modulation of corticostriatal synaptic plasticity.

In PD, the loss of dopaminergic input to the basal ganglia causes the sensitization of D1R transmission, which potentiates the effects of dopaminergic drugs on dSPN [2,3,11,12,14,33]. In line with this, we show that the L-DOPA-induced increase in JNK and cJun phosphorylation occurs in combination with dopamine depletion. A similar mode of regulation has been described for other signaling pathways, including the cAMP cascade, ERK, and the mammalian target of rapamycin, which participate in the actions of drugs against Parkinson's disease [9,11,13,14,34-36]. It should be noted that a previous study carried out in the rat 6-OHDA-lesion model of PD did not show any modifications in the state of phosphorylation of JNK, in response to L-DOPA [37]. This discrepancy may depend on species-specific differences (rat vs. mouse). Moreover, the present study shows a maximal phosphorylation of JNK at 15 min following administration of L-DOPA. In contrast, in the previous study JNK phosphorylation was examined 45 min after L-DOPA, a time at which, in the rat, the effect of D1R activation on P-JNK may have subsided cf. [20].

One of the primary effects of stimulation of D1Rs in SPNs is the phosphorylation of DARPP-32 on Thr34, which is catalyzed by PKA. This phosphorylation converts DARPP-32 into an inhibitor of PP-1 and plays a critical role in a wide range of responses to dopaminergic drugs [27]. Our results indicate that L-DOPA-induced JNK signaling requires the stimulation of the PKA/DARPP-32 signaling cascade, which leads to suppression of PP-1 activity. Thus, in T34A DARPP-32 mutant mice, lack of inhibitory control of PP-1 largely prevents L-DOPA-mediated increases in JNK phosphorylation. Previous work in human monocytes has pointed to PP-2A as the main phosphatase involved in the regulation of JNK

during acute inflammation [38]. The present data suggest that, in the brain, PP-1 is an additional phosphatase implicated in dopamine-mediated control of JNK signaling.

The effect of DARPP-32 inactivation on the phosphorylation of cJun is less prominent than that observed on JNK. This suggests that following D1R sensitization, abnormal activation of PKA, which is upstream of DARPP-32, may be sufficient to increase cJun phosphorylation independently of parallel inhibition of PP-1. It is also possible that the residual phosphorylation of JNK and Ras/ERK [9] still observed after genetic inactivation of DARPP-32 may concur to maintain cJun in a partially active state. Future studies will be needed to examine these possibilities.

Stimulation of mitogen-activated protein kinases typically depends on NMDA receptor transmission. For instance, increased ERK phosphorylation in response to dopaminergic drugs, such as cocaine and amphetamine, is reduced by blockade of NMDA receptors [29,30]. NMDA receptors have also been implicated in stress-induced activation of JNK [31]. In contrast to these observations, the L-DOPA-induced increase in JNK and cJun phosphorylation in the dopamine-depleted striatum is unaffected by the NMDA receptor antagonist, MK-801. These results suggest that in PD, the loss of dopamine input to the striatum produces a sensitization that allows D1Rs to promote JNK/cJun signaling independently of NMDA receptor transmission.

The D1R-driven stimulation of JNK occurs specifically in dSPN. Activation of these neurons suppresses the inhibitory control exerted by the basal ganglia on thalamo-cortical neurons, thus promoting motor activity [39-41]. In dSPN, dopamine via D1Rs activates postsynaptic signaling cascades (e.g. ERK cascade) that increase synaptic strength [26,42]. This postsynaptic potentiation counteracts the presynaptic inhibition of glutamate release by adenosine A1 receptors, thereby creating a dynamic balance between LTD and LTP mechanisms [26]. The present results show that, in PD mice, JNK activation contributes to the D1R-mediated effects at corticostriatal synapses on dSPN, pointing to a role for JNK signaling in the regulation of striatal synaptic plasticity. Notably, this regulation is absent in naïve mice and occurs only in a PD model, characterized by the loss of dopaminergic input to the

striatum. Dopamine depletion has been linked to the development of sensitization at D1R. The present study indicates that this pathological condition acts as a functional switch by conferring on JNK abnormal signaling properties, potentially linked to the actions of anti-parkinsonian medications.

D1R sensitization and loss of synaptic downscaling are regarded as causal factors in the development of aberrant motor responses produced by L-DOPA, such as dyskinesia [3,43,44]. Therefore, the attenuation of D1R transmission produced by JNK inhibitors and their permissive action on LTD may help to control this serious complication. In line with this possibility, it has been shown that overexpression in dSPN of ΔcJun, a truncated form of cJun which lacks transcriptional activity, attenuates L-DOPA-induced dyskinesia [45]. Recent studies show that administration of L-DOPA increases spine volume and postsynaptic density (PSD) length, in the dSPN of dyskinetic mice [46,47]. Interestingly, D1R-mediated activation of JNK may participate in this phenomenon, since JNK has been shown to increase the synaptic content of PSD-95 [48].

In conclusion, this study supports the involvement of the JNK signaling pathway in dopamine transmission. In particular, we show that depletion of dopamine, a pathological hallmark of PD, confers on dopaminergic drugs the ability to activate JNK. This effect occurs in a well-defined population of SPNs and is causally linked to synaptic responses produced by D1R activation. These findings shed new light on the mechanisms by which anti-Parkinson's drugs modify basal ganglia transmission and provide critical information for the development of novel approaches for the treatment of PD.

Acknowledgements

This work was supported by the Swedish Research Council, Parkinson Foundation in Sweden and Swedish Brain Foundation (to GF), and by Fondazione Istituto Italiano di Tecnologia, Compagnia di San Paolo and Fondazione Cariplo (to RT).

References

1. Kebabian JW, Calne DB (1979) Multiple receptors for dopamine. Nature 277: 93-96.

2. Aubert I, Guigoni C, Hakansson K, Li Q, Dovero S, et al. (2005) Increased D1 dopamine receptor signaling in levodopa-induced dyskinesia. Ann Neurol 57: 17-26.

3. Feyder M, Bonito-Oliva A, Fisone G (2011) L-DOPA-induced dyskinesia and abnormal signaling in striatal medium spiny neurons: focus on dopamine D1 receptor-mediated transmission. Front Behav Neurosci 5: 71.

4. Gerfen CR, Engber TM, Mahan LC, Susel Z, Chase TN, et al. (1990) D1 and D2 dopamine receptor-regulated gene expression of striatonigral and striatopallidal neurons. Science 250: 1429-1432.

5. Berthet A, Porras G, Doudnikoff E, Stark H, Cador M, et al. (2009) Pharmacological analysis demonstrates dramatic alteration of D1 dopamine receptor neuronal distribution in the rat analog of L-DOPA-induced dyskinesia. J Neurosci 29: 4829-4835.

6. Corvol JC, Muriel MP, Valjent E, Feger J, Hanoun N, et al. (2004) Persistent increase in olfactory type G-protein alpha subunit levels may underlie D1 receptor functional hypersensitivity in Parkinson disease. J Neurosci 24: 7007-7014.

7. Guigoni C, Doudnikoff E, Li Q, Bloch B, Bezard E (2007) Altered D(1) dopamine receptor trafficking in parkinsonian and dyskinetic non-human primates. Neurobiol Dis 26: 452-463.

8. Rangel-Barajas C, Silva I, Lopez-Santiago LM, Aceves J, Erlij D, et al. (2011) l-DOPA-induced dyskinesia in hemiparkinsonian rats is associated with up-regulation of adenylyl cyclase type V/VI and increased GABA release in the substantia nigra reticulata. Neurobiol Dis 41: 51-61.

9. Santini E, Valjent E, Usiello A, Carta M, Borgkvist A, et al. (2007) Critical involvement of cAMP/DARPP-32 and extracellular signal-regulated protein kinase signaling in L-DOPA-induced dyskinesia. J Neurosci 27: 6995-7005.

10. Gerfen CR, Miyachi S, Paletzki R, Brown P (2002) D1 dopamine receptor supersensitivity in the dopamine-depleted striatum results from a switch in the regulation of ERK1/2/MAP kinase. J Neurosci 22: 5042-5054.

11. Pavon N, Martin AB, Mendialdua A, Moratalla R (2006) ERK phosphorylation and FosB expression are associated with L-DOPA-induced dyskinesia in hemiparkinsonian mice. Biol Psychiatry 59: 64-74.

12. Santini E, Alcacer C, Cacciatore S, Heiman M, Herve D, et al. (2009) L-DOPA activates ERK signaling and phosphorylates histone H3 in the striatonigral medium spiny neurons of hemiparkinsonian mice. J Neurochem 108: 621-633.

13. Westin JE, Vercammen L, Strome EM, Konradi C, Cenci MA (2007) Spatiotemporal pattern of striatal ERK1/2 phosphorylation in a rat model of L-DOPA-induced dyskinesia and the role of dopamine D1 receptors. Biol Psychiatry 62: 800-810.

14. Santini E, Valjent E, Fisone G (2010) mTORC1 signaling in Parkinson's disease and L-DOPA-induced dyskinesia: A sensitized matter. Cell Cycle 9: 2713-2718.

15. Coffey ET (2014) Nuclear and cytosolic JNK signalling in neurons. Nat Rev Neurosci 15: 285-299.

16. Manning AM, Davis RJ (2003) Targeting JNK for therapeutic benefit: from junk to gold? Nat Rev Drug Discov 2: 554-565.

17. Derijard B, Hibi M, Wu IH, Barrett T, Su B, et al. (1994) JNK1: a protein kinase stimulated by UV light and Ha-Ras that binds and phosphorylates the c-Jun activation domain. Cell 76: 1025-1037.

18. Papavassiliou AG, Treier M, Bohmann D (1995) Intramolecular signal transduction in c-Jun. EMBO J 14: 2014-2019.

19. Zhen X, Uryu K, Wang HY, Friedman E (1998) D1 dopamine receptor agonists mediate activation of p38 mitogen-activated protein kinase and c-Jun amino-terminal kinase by a protein kinase A-dependent mechanism in SK-N-MC human neuroblastoma cells. Mol Pharmacol 54: 453-458.

20. Go BS, Ahn SM, Shim I, Choe ES (2010) Activation of c-Jun N-terminal kinase is required for the regulation of endoplasmic reticulum stress response in the rat dorsal striatum following repeated cocaine administration. Neuropharmacology 59: 100-106.

21. Gong S, Zheng C, Doughty ML, Losos K, Didkovsky N, et al. (2003) A gene expression atlas of the central nervous system based on bacterial artificial chromosomes. Nature 425: 917-925.

22. Svenningsson P, Tzavara ET, Carruthers R, Rachleff I, Wattler S, et al. (2003) Diverse psychotomimetics act through a common signaling pathway. Science 302: 1412-1415.

23. Toth ZE, Mezey E (2007) Simultaneous visualization of multiple antigens with tyramide signal amplification using antibodies from the same species. J Histochem Cytochem 55: 545-554.

24. Fino E, Glowinski J, Venance L (2005) Bidirectional activity-dependent plasticity at corticostriatal synapses. J Neurosci 25: 11279-11287.

25. Nazzaro C, Greco B, Cerovic M, Baxter P, Rubino T, et al. (2012) SK channel modulation rescues striatal plasticity and control over habit in cannabinoid tolerance. Nat Neurosci 15: 284-293.

26. Trusel M, Cavaccini A, Gritti M, Greco B, Saintot PP, et al. (2015) Coordinated Regulation of Synaptic Plasticity at Striatopallidal and Striatonigral Neurons Orchestrates Motor Control. Cell Rep 13: 1353-1365.

27. Greengard P (2001) The neurobiology of slow synaptic transmission. Science 294: 1024-1030.

28. Cahill E, Pascoli V, Trifilieff P, Savoldi D, Kappes V, et al. (2014) D1R/GluN1 complexes in the striatum integrate dopamine and glutamate signalling to control synaptic plasticity and cocaine-induced responses. Mol Psychiatry 19: 1295-1304.

29. Valjent E, Corvol JC, Pages C, Besson MJ, Maldonado R, et al. (2000) Involvement of the extracellular signal-regulated kinase cascade for cocaine-rewarding properties. J Neurosci 20: 8701-8709.

30. Valjent E, Pascoli V, Svenningsson P, Paul S, Enslen H, et al. (2005) Regulation of a protein phosphatase cascade allows convergent dopamine and glutamate signals to activate ERK in the striatum. Proc Natl Acad Sci U S A 102: 491-496.

31. Mukherjee PK, DeCoster MA, Campbell FZ, Davis RJ, Bazan NG (1999) Glutamate receptor signaling interplay modulates stress-sensitive mitogen-activated protein kinases and neuronal cell death. J Biol Chem 274: 6493-6498.

32. Zhang T, Inesta-Vaquera F, Niepel M, Zhang J, Ficarro SB, et al. (2012) Discovery of potent and selective covalent inhibitors of JNK. Chem Biol 19: 140-154.

33. Darmopil S, Martin AB, De Diego IR, Ares S, Moratalla R (2009) Genetic inactivation of dopamine D1 but not D2 receptors inhibits L-DOPA-induced dyskinesia and histone activation. Biol Psychiatry 66: 603-613.

34. Ruiz-DeDiego I, Mellstrom B, Vallejo M, Naranjo JR, Moratalla R (2015) Activation of DREAM (downstream regulatory element antagonistic modulator), a calcium-binding protein, reduces L-DOPA-induced dyskinesias in mice. Biol Psychiatry 77: 95-105.

35. Solis O, Garcia-Montes JR, Gonzalez-Granillo A, Xu M, Moratalla R (2017) Dopamine D3 Receptor Modulates l-DOPA-Induced Dyskinesia by Targeting D1 Receptor-Mediated Striatal Signaling. Cereb Cortex 27: 435-446.

36. Subramaniam S, Napolitano F, Mealer RG, Kim S, Errico F, et al. (2011) Rhes, a striatal-enriched small G protein, mediates mTOR signaling and L-DOPA-induced dyskinesia. Nat Neurosci 15: 191-193.

37. Ahmed MR, Bychkov E, Kook S, Zurkovsky L, Dalby KN, et al. (2015) Overexpression of GRK6 rescues L-DOPA-induced signaling abnormalities in the dopamine-depleted striatum of hemiparkinsonian rats. Exp Neurol 266: 42-54.

38. Shanley TP, Vasi N, Denenberg A, Wong HR (2001) The serine/threonine phosphatase, PP2A: endogenous regulator of inflammatory cell signaling. J Immunol 166: 966-972.

39. Albin RL, Young AB, Penney JB (1989) The functional anatomy of basal ganglia disorders. Trends Neurosci 12: 366-375.

40. DeLong MR (1990) Primate models of movement disorders of basal ganglia origin. Trends Neurosci 13: 281-285.

41. Gerfen CR (1992) The neostriatal mosaic: multiple levels of compartmental organization in the basal ganglia. Annu Rev Neurosci 15: 285-320.

42. Cerovic M, Bagetta V, Pendolino V, Ghiglieri V, Fasano S, et al. (2015) Derangement of Ras-guanine nucleotide-releasing factor 1 (Ras-GRF1) and extracellular signal-regulated kinase (ERK) dependent striatal plasticity in L-DOPA-induced dyskinesia. Biol Psychiatry 77: 106-115.

43. Guigoni C, Aubert I, Li Q, Gurevich VV, Benovic JL, et al. (2005) Pathogenesis of levodopa-induced dyskinesia: focus on D1 and D3 dopamine receptors. Parkinsonism Relat Disord 11 Suppl 1: S25-29.

44. Calabresi P, Pisani A, Rothwell J, Ghiglieri V, Obeso JA, et al. (2016) Hyperkinetic disorders and loss of synaptic downscaling. Nat Neurosci 19: 868-875.

45. Feyder M, Sodersten E, Santini E, Vialou V, LaPlant Q, et al. (2016) A Role for Mitogen- and Stress-Activated Kinase 1 in L-DOPA-Induced Dyskinesia and FosB Expression. Biol Psychiatry 79: 362-371.

46. Suarez LM, Solis O, Aguado C, Lujan R, Moratalla R (2016) L-DOPA Oppositely Regulates Synaptic Strength and Spine Morphology in D1 and D2 Striatal Projection Neurons in Dyskinesia. Cereb Cortex 26: 4253-4264.

47. Suarez LM, Solis O, Carames JM, Taravini IR, Solis JM, et al. (2014) L-DOPA treatment selectively restores spine density in dopamine receptor D2-expressing projection neurons in dyskinetic mice. Biol Psychiatry 75: 711-722.

48. Kim MJ, Futai K, Jo J, Hayashi Y, Cho K, et al. (2007) Synaptic accumulation of PSD-95 and synaptic function regulated by phosphorylation of serine-295 of PSD-95. Neuron 56: 488-502.

49. Franklin KBJ, Paxinos G (1997) The Mouse Brain in Stereotaxic Coordinates. San Diego: Academic Press.

Legends to the figures

Fig 1. L-DOPA triggers JNK and cJun phosphorylation in SPNs of hemiparkinsonian mice.

Mice with a unilateral injection of 6-OHDA in the MFB were treated with either saline or L-DOPA (10 mg/kg) and perfused after 15, 30, 60 or 120 min. (A) Coronal section of mouse brain immunostained for TH [AP +0.26 mm from the bregma [49]]. Note the loss of dopaminergic innervation, assessed as lack of TH-immunoreactivity, produced by 6-OHDA in the striatum ipsilateral to the lesion. Squares indicate the regions of the DLS selected for the immunohistochemical analysis. Scale bar, 500 μm. (B,C) Confocal images (20X) showing P-JNK (B) and P-cJun (C) immunoreactive cells in the striata contralateral (control) or ipsilateral (lesion) to the side of the 6-OHDA lesion in saline and L-DOPA treated mice at 30 min. Scale bar, 50 μm. (D,E) Quantification of P-JNK (D) and P-cJun (E) positive cells/100 mm^2 . Bar diagrams (left panels) show the increase induced by the lesion 30 min after L-DOPA; line graphs (right panels) show the time course of the effect of L-DOPA. Data are expressed as mean ± S.E.M. 2W ANOVA indicated a significant lesion x treatment interaction ($F_{1,8}$ = 95.74, $p < 0.0001$ for P-JNK; $F_{1,8}$ = 185.7, $p < 0.0001$ for P-cJun; n = 3 mice/group) and lesion x time interaction ($F_{3,16}$ = 15.92, $p < 0.0001$ for P-JNK; $F_{3,16}$ = 6.629, $p = 0.004$ for P-cJun; n = 3 mice /group). * $p < 0.0001$ for 6-OHDA lesion treated with L-DOPA vs. saline-Control, saline-6-OHDA and L-DOPA-Control groups (*Tukey*).

Fig 2. Activation of JNK signaling occurs in D1R-expressing SPNs.

Drd1a-EGFP and *Drd2a*-EGFP mice with a unilateral injection of 6-OHDA in the MFB were treated with L-DOPA (10 mg/kg) and perfused after 30 min. (A,B) Confocal images (20X) of control and 6-OHDA-lesion striata double-stained for EGFP and P-JNK (A), or EGFP and P-cJun (B). Note the co-localization of P-JNK and P-cJun with EGFP in *Drd1a*-EGFP mice ($F_{2,2}$ = 118.9, $p = 0.0005$ for P-JNK and $F_{2,2}$ = 1194 $p = 0.0012$ for P-cJun, t-test; n = 3 mice) and the distinct fluorescent signals in *Drd2a*-EGFP mice ($F_{2,2}$ = 804.3, $p = 0.0002$ for P-JNK and $F_{2,2}$ = 1230, $p = 0.0007$ for P-cJun, t-test; n = 3 mice).

Scale bar, 50 μm. Pie charts show the percentage of cells in which EGFP-immunoreactivity (green) colocalizes (orange) with P-JNK (A) and P-cJun (B) (red). (C) Confocal images (40 and 63X) from a *Drd2a*-EGFP mouse, showing triple staining for EGFP (green), P-JNK (blue) and P-cJun (red) in the striatum ipsilateral to the 6-OHDA-lesion. The inset shows co-localization (purple) between P-JNK and P-cJun immunoreactivity in double-labeled cells devoid of EGFP fluorescent signal (i.e. dSPN). Scale bar, 20 μm.

Fig 3. Phosphorylation of JNK and cJun is prevented by SCH23390 and induced by SKF38393 treatments in the dopamine depleted striatum.

Mice with a unilateral injection of 6-OHDA in the MFB were either treated with SCH23390 (0.2 mg/Kg; 15 min prior to L-DOPA) and perfused 30 min after L-DOPA administration or treated with SKF38393 (10 mg/Kg) and perfused after 30 min. (A,C) Confocal images (20X) showing P-JNK (A,E) and P-cJun (C,G) in the striata contralateral (control) or ipsilateral (lesion) to the side of the 6-OHDA lesion. (B,D,F,H) Bar diagrams representing the number of P-JNK (B,F) and P-cJun (D,H) immunoreactive cells/100 mm^2 in the control and 6-OHDA striata of mice treated with L-DOPA (B,D) or SKF38393 (F,H) and in the 6-OHDA striatum of mice treated with L-DOPA + SCH23390 (B,D). Scale bar, 50 μm. Data are expressed as mean ± S.E.M. 2W ANOVA indicated significant lesion x treatment interaction ($F_{1,8}$ = 46.94, p = 0.0001 for P-JNK; $F_{1,12}$ = 8.852, p = 0.0116 for P-cJun; n = 3 mice/group). t-test indicated significant difference between 6-OHDA lesion and Control treated with SKF38393 ($F_{2,2}$ = 1381, p < 0.0001 for P-JNK; $F_{2,2}$ = 1630, p = 0.0001 for P-cJun; n = 3 mice/group). * p < 0.001 for 6-OHDA lesion treated with L-DOPA vs. Control treated with L-DOPA (*Tukey*); † p = 0.0055 and †† p < 0.0001 for 6-OHDA lesion treated with L-DOPA + SCH23390 vs. 6-OHDA lesion treated with L-DOPA (*Tukey*). # p ≤ 0.0001 (t-test).

Fig 4. L-DOPA-mediated regulation of JNK depends on cAMP/DARPP-32 signaling and does not require NMDA receptor transmission. (A-D) Wildtype and DARPP-32 T34A mutant mice with a unilateral injection of 6-OHDA in the MFB were treated with L-DOPA (10 mg/kg) and perfused after 30 min. (E-H) Mice with a unilateral 6-OHDA lesion in the MFB were treated with MK-801 (0.15 mg/Kg; 30 min prior to L-DOPA) and perfused 30 min after administration of L-DOPA. (A,C,E,G) Confocal images (20X) showing P-JNK (A) and P-cJun (C) immunoreactive cells in the striata contralateral (control) or ipsilateral (lesion) to the side of the 6-OHDA lesion. Scale bar, 50 μm. (B,D) Bar diagrams representing the number of P-JNK (B) and P-cJun (D) immunoreactive cells/100 mm^2. Note the reduction of the effect of L-DOPA in the 6-OHDA-lesion striatum of DARPP-32 T34A mutant mice compared to wildtype mice. Data are expressed as means ± S.E.M. 2W ANOVA indicated significant lesion x genotype interaction ($F_{1,12}$ = 53.92, $p < 0.0001$ for P-JNK; $F_{1,11}$ = 10.02 $p = 0.009$ for P-cJun; n = 4 mice/group). (F,H) Bar diagrams representing the number of P-JNK (F) and P-cJun (H) immunoreactive cells/100 mm^2 in the control and 6-OHDA striata of mice treated with L-DOPA and in the 6-OHDA striatum of mice treated with L-DOPA + MK801. Data are expressed as mean ± S.E.M. 2W ANOVA indicated significant effect of the lesion ($F_{1,8}$ = 204.1, $p < 0.0001$ for P-JNK; $F_{1,8}$ = 207.8, $p < 0.0001$ for P-cJun; n = 3 mice/group) and no significant lesion x treatment interaction ($p > 0.05$ for both P-JNK and P-cJun) * $p < 0.001$ for 6-OHDA lesion wildtype treated with L-DOPA vs. Control wildtype treated with L-DOPA (*Tukey*); † $p = 0.005$ and †† $p < 0.0001$ for 6-OHDA lesion DARPP-32 T34A treated with L-DOPA vs. 6-OHDA lesion wildtype treated with L-DOPA (*Tukey*).

Fig 5. D1R-mediated modulation of long-term synaptic depression (LTD) at cortical connections to dSPN of 6-OHDA-lesioned mice.

(A) (Top left) Experimental configuration in horizontal brain slices containing the dorsolateral striatum. (Bottom Left) High frequency stimulation (HFS) of Layer 5 cortical afferents resulted in LTD of excitatory postsynaptic responses in dSPN 6-OHDA mice (1W RM ANOVA, $F_{7,22}$ = 15, $p = 0.0003$, n =

8 slices from 6 mice; $p < 0.05$, *Tukey*). This form of HFS-LTD was blocked by bath application of the A1R antagonists DPCPX (500 nM, light blue bar) (1W RM ANOVA, $F_{4,22} = 0.5$, $p = 0.6$, n = 5 slices from 4 mice; dSPN 6-$OHDA_{ipsi}$ vs. dSPN 6-$OHDA_{ipsi}$ + DPCPX, $p = 0.04$, t-test). (B) Stimulation of dSPN with L-DOPA (10 μM; grey bar) or with the D1R agonist SKF38393 (3 μM; black bar) negatively modulated HFS-LTD at dSPN 6-OHDA synapses (1W RM ANOVA, dSPN 6-$OHDA_{ipsi}$ + L-DOPA, $F_{4,22} = 2$, $p = 0.2$, n = 5 slices from 4 mice; dSPN 6-$OHDA_{ips}$ + SKF3839, $F_{5,22} = 5$, $p = 0.02$, n = 6 slices from 5 mice; $p > 0.05$, *Tukey*; 1W ANOVA, $F_{2,16} = 6$, $p = 0.02$; dSPN 6-$OHDA_{ipsi}$ vs. dSPN 6-$OHDA_{ipsi}$ + L-DOPA, $p = 0.04$, *Dunnet*; dSPN 6-$OHDA_{ipsi}$ vs. dSPN 6-$OHDA_{ipsi}$ + SKF3839, $p = 0.01$, *Dunnet*). Black line in (B) indicates HFS-LTD in dSPN 6-OHDA mice, as reported in (A); (A,B) (Top right) Schematic of proposed signaling elements targeted by the defined antagonist. (Bottom left) Data are presented as normalized EPSP amplitude and normalized R_{inp} (mean ± S.E.M). (Bottom right) Plot of ratios of synaptic responses after (a) and before (b) the HFS. Insets: (left) superimposed averaged recordings (ten traces) before (black line) and after (blue line) the delivery of the HFS protocol (blue vertical bar). * $p < 0.05$ (t-test/*Dunnet*).

Fig 6. JNK signaling activation mediates the synaptic effect of D1R activation in PD but not in control mice.

(A) In PD mice, D1R-mediated synaptic inhibition of LTD was averted by including the JNK inhibitors SP600125 (10 μM) or JNK-IN-8 (1 μM) in the postsynaptic dSPN (1W RM ANOVA, dSPN 6-$OHDA_{ipsi}$ + SKF38393/SP600125, $F_{5,22} = 15$, $p = 0.0001$, n = 6 slices from 5 mice; $p < 0.05$, *Tukey*; dSPN 6-$OHDA_{ipsi}$ + SKF38393/JNK-IN-8, $F_{4,22} = 5$, $p < 0.0001$, n = 5 slices from 4 mice; $p < 0.05$, *Tukey*; 1W ANOVA, $F_{14,2} = 9$, $p = 0.002$; $p < 0.01$; dSPN 6-$OHDA_{ipsi}$ + SKF3839 vs. dSPN 6-$OHDA_{ipsi}$ + SKF38393/SP600125, $p = 0.04$, *Dunnet*; dSPN 6-$OHDA_{ipsi}$ + SKF3839 vs. dSPN 6-$OHDA_{ipsi}$ + SKF38393/JNK-IN-8, $p = 0.001$, *Dunnet*). Blue line indicates plasticity in dSPN 6-OHDA mice upon SKF38393 application as reported in Fig. 5A. (B) Striatal slices from 6-OHDA-lesion mice were

incubated for 5 min with vehicle, SKF38393 (3 μM), or SKF38393 in the presence of SP600125 (20 μM) or JNK-IN-8 (10 μM). P-cJun and P-ERK 1/2 were determined by Western blotting (25 and 10 μg of protein were loaded, respectively). Note the reduction of SKF38393-induced P-cJun produced by the two JNK inhibitors (top panels). In contrast, SP600125 and JNK-IN-8 did not affect the increase in P-ERK produced by SKF38393 (bottom panels). Summary of data were calculated as percentage of control and are represented as mean ± S.E.M. 1W ANOVA indicated significant effect of the treatment for both P-cJun ($F_{3,16}$ = 15.22, $p < 0.0001$, n = 5 slices from 5 mice) and P-ERK 1/2 ($F_{3,16}$ = 18.23, $p < 0.0001$, n = 5 slices from mice). (C) In naïve mice, the JNK inhibitor JNK-IN-8 (1 μM) did not prevent SKF38393 from reducing HFS-LTD (1W RM ANOVA, dSPN Naive, $F_{5,22}$ = 10, p = 0.0005, n = 6 from 5 mice; $p < 0.05$, *Tukey*; dSPN Naive + SKF38393, $F_{5,22}$ = 1.7, p = 0.2, n = 6 slices from 6 mice; dSPN Naive + SKF38393/JNK-IN-8, $F_{5,22}$ =1.2, p = 0.3, n = 6 slices from 4 mice; 1W ANOVA, $F_{2,15}$ = 7, p = 0.008; dSPN Naive vs. dSPN Naive + SKF38393, p = 0.02, *Dunnet*; dSPN Naive + SKF3839 vs. dSPN Naïve + SKF38393/JNK-IN-8, p = 0.01, *Dunnet*). (A,C) (Bottom left) Data are presented as normalized EPSP amplitude and normalized R_{inp} (mean ± S.E.M). (Bottom right) Plot of ratios of synaptic responses after (a) and before (b) the HFS. (Top left) Superimposed averaged recordings (ten traces) before (black line) and after (blue line) the delivery of the HFS protocol (blue vertical bar). (Top right) schematic of proposed signaling elements targeted by the defined agonists or inhibitors. * $p < 0.05$ (*Dunnet*); ** $p < 0.01$ (*Dunnet*); # $p < 0.01$ for SKF38393 vs. Vehicle (*Tukey*); † p = 0.02 for SKF38393 vs. SKF38393 + SP600125 (*Tukey*); †† $p < 0.0001$ for SKF38393 vs. SKF38393 + JNK-IN-8 (*Tukey*).

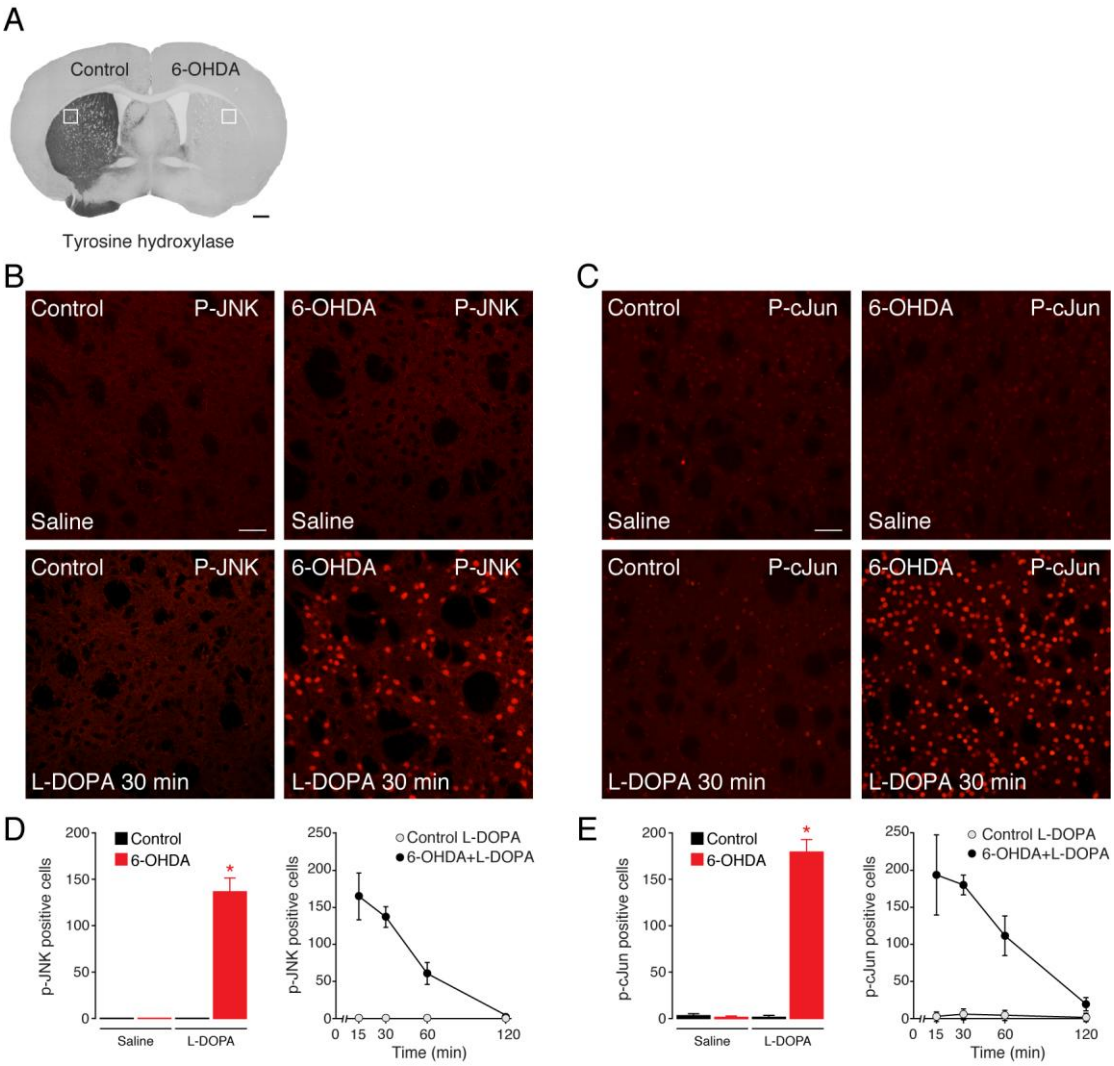

Fig. 1

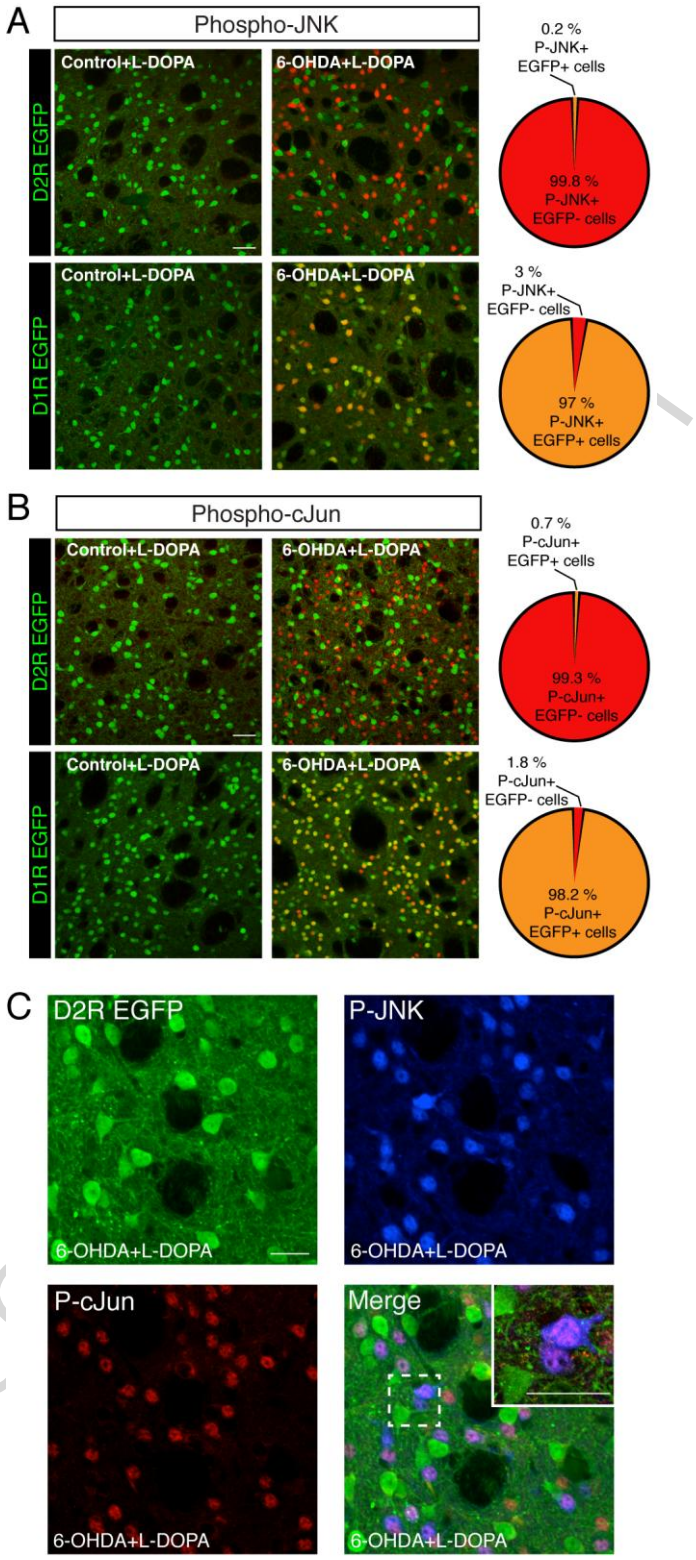

Fig. 2

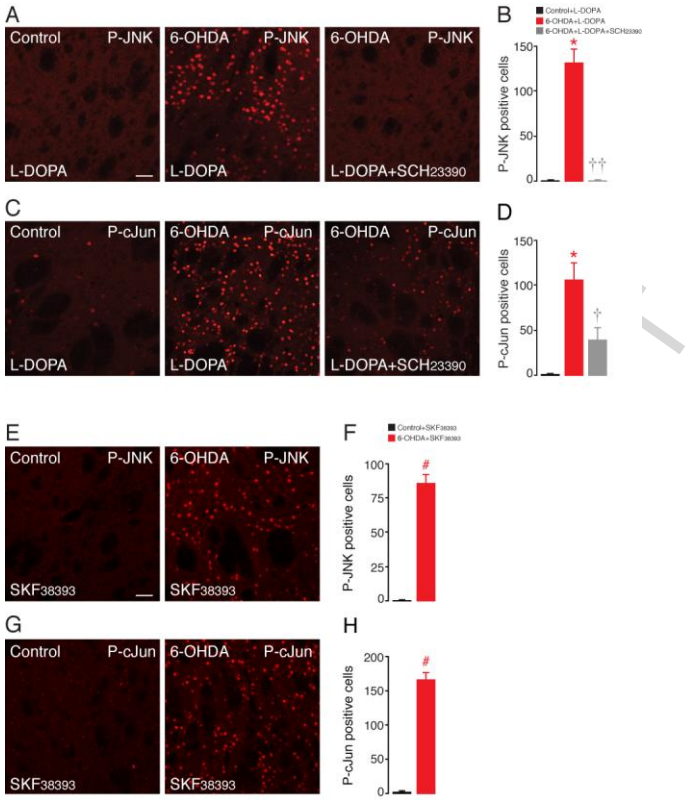

Fig. 3

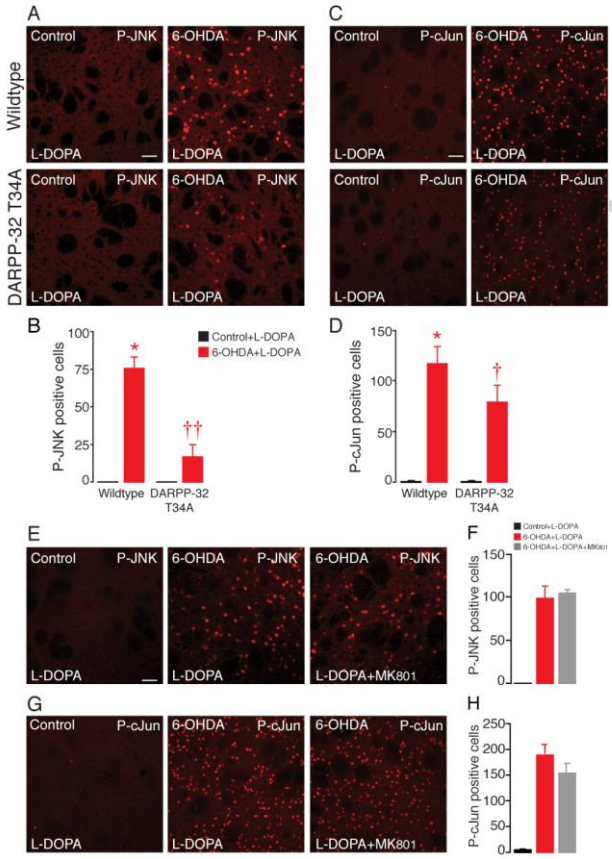

Fig. 4

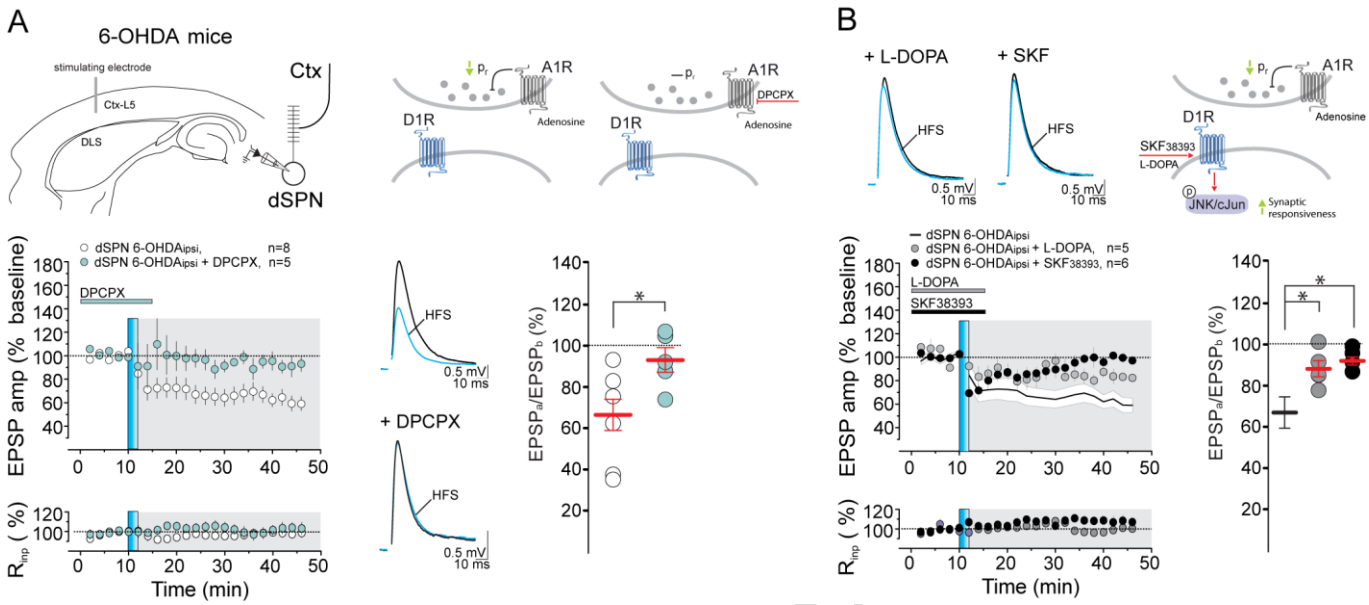

Fig. 5

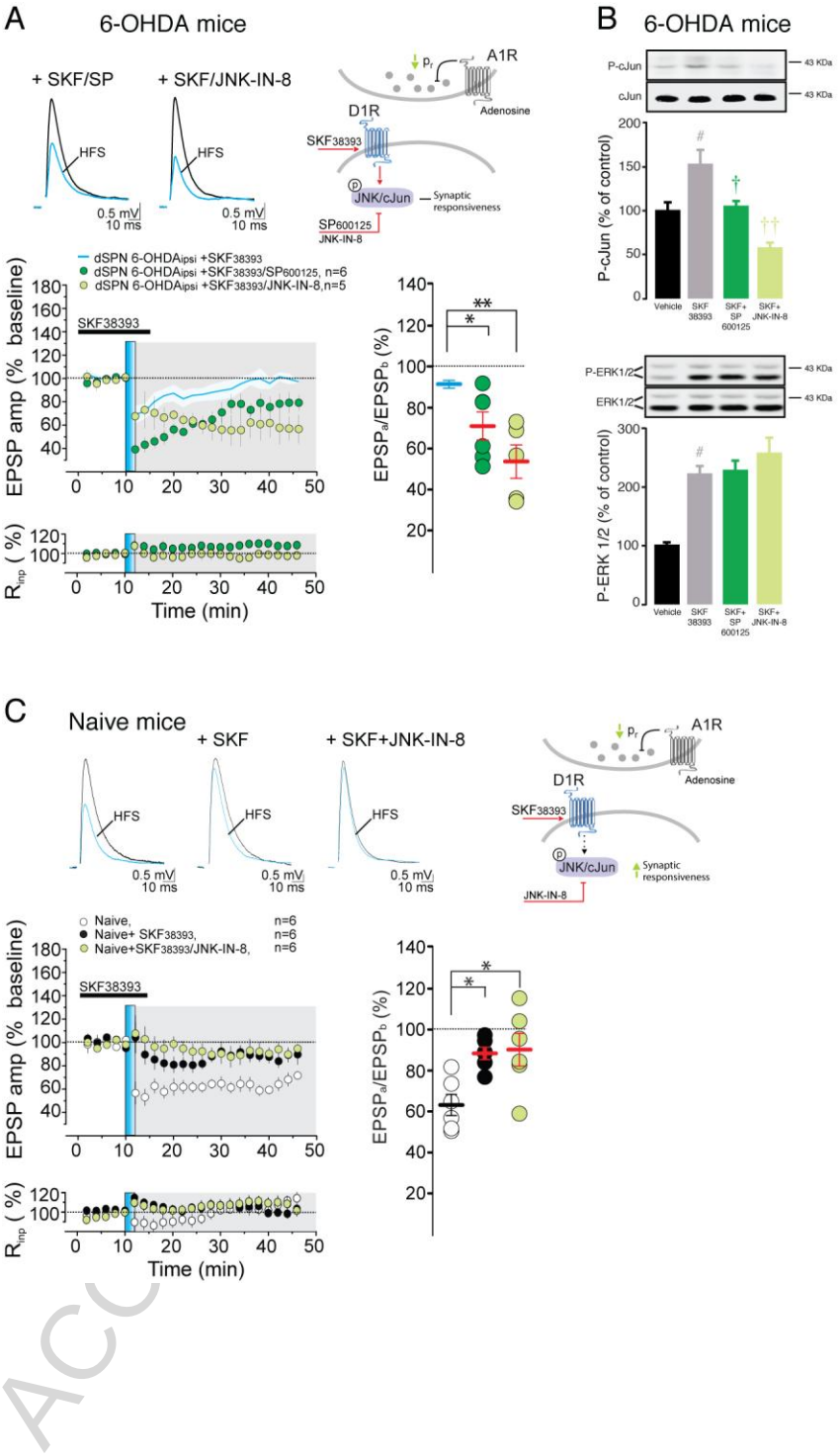

Fig. 6

Highlights

- Administration of L-DOPA promotes JNK signaling in a mouse model of Parkinson's disease
- This effect depends on D1R-mediated activation of DARPP-32 and occurs selectively in dSPNs
- JNK is required for D1R-mediated regulation of synaptic plasticity in experimental parkinsonism